Ann. Geophys., 34, 85–89, 2016
www.ann-geophys.net/34/85/2016/
doi:10.5194/angeo-34-85-2016

Annales Geophysicae Open Access EGU

Ion Bernstein waves in the magnetic reconnection region

Y. Narita[1,2], R. Nakamura[1], W. Baumjohann[1], K.-H. Glassmeier[2,3], U. Motschmann[4,5], and H. Comişel[4,6]

[1]Space Research Institute, Austrian Academy of Sciences, Schmiedlstr. 6, 8042 Graz, Austria
[2]Institut für Geophysik und extraterrestrische Physik, Technische Universität Braunschweig, Mendelssohnstr. 3, 38106 Braunschweig, Germany
[3]Max-Planck-Institut für Sonnensystemforschung, Justus-von-Liebig-Weg 3, 37077 Göttingen, Germany
[4]Institut für Theoretische Physik, Technische Universität Braunschweig, Mendelssohnstr. 3, 38106 Braunschweig, Germany
[5]Deutsches Zentrum für Luft- und Raumfahrt, Institut für Planetenforschung, Rutherfordstr. 2, 12489 Berlin, Germany
[6]Institute for Space Sciences, Atomiştilor 409, P.O. Box MG-23, Bucharest-Măgurele, 077125, Romania

Correspondence to: Y. Narita (yasuhito.narita@oeaw.ac.at)

Received: 2 December 2015 – Accepted: 12 January 2016 – Published: 21 January 2016

Abstract. Four-dimensional energy spectra and a diagram for dispersion relations are determined for the first time in a magnetic reconnection region in the magnetotail using data from four-spacecraft measurements by the Cluster mission on a spatial scale of 200 km, about 0.1 ion inertial lengths. The energy spectra are anisotropic with an extension in the perpendicular direction and axially asymmetric with respect to the mean magnetic field. The dispersion diagram in the plasma rest frame is in reasonably good agreement with the ion Bernstein waves at the second and higher harmonics of the proton gyrofrequency. Perpendicular-propagating ion Bernstein waves likely exist in an outflow region of magnetic reconnection, which may contribute to bifurcation of the current sheet in the outflow region.

Keywords. Magnetospheric physics (magnetotail) – space plasma physics (magnetic reconnection; turbulence)

1 Introduction

Magnetic reconnection in collisionless plasmas, as realized by auroral substorms in the Earth magnetosphere and solar eruptions (flares and coronal mass ejections), often exhibits wave activity. Two competing ideas exist on the role of waves in reconnection. First, waves can trigger magnetic reconnection through the anomalous resistivity caused by enhanced electrostatic fluctuations such as the Buneman instability, the ion acoustic mode, and the lower hybrid drift instability and through pitch angle scattering by electromagnetic fluctuations such as kinetic Alfvén waves and whistler waves (see review in Treumann, 2001). Second, waves are driven by reconnection and serve as an efficient dissipation channel of the energy conversion process in magnetic reconnection such as whistler waves associated with the reconnection outflow (Fujimoto and Sydora, 2008; Eastwood et al., 2009). While recent spacecraft observations indicate the existence of whistler waves (Eastwood et al., 2009) and lower hybrid drift waves (Norgren et al., 2012) in thin current sheets, these data analyses are limited to various assumptions, e.g., single wave mode at one frequency, associated with single- or two-point measurements in space. A proper, unambiguous characterization of the waves in the reconnection region is achieved with at least four-point measurements, allowing us to determine the wave modes and the energy spectra in the wavevector and frequency domains.

Here we present for the first time evidence for ion Bernstein waves in a magnetic reconnection region in the Earth magnetotail. The analysis makes extensive use of four-spacecraft measurements performed in situ by the Cluster mission (Escoubet et al., 2001) to directly determine the energy spectra in the four-dimensional Fourier domain spanning the frequencies and the wavevectors as well as to determine the diagram for dispersion relation. Ion Bernstein waves in a magnetic reconnection region have so far largely been overlooked. We propose the ion Bernstein mode to be an essential ingredient of the magnetic reconnection process in space and astrophysical collisionless plasmas.

Published by Copernicus Publications on behalf of the European Geosciences Union.

AnGeo Communicates

2 Data analysis

2.1 Cluster observation

On 24 August 2003, 18:30–18:50 UT, Cluster encountered a thin current sheet in the Earth magnetotail from the Northern to the Southern Hemisphere at a distance of about 17 Earth radii (Fig. 1). The observed current sheet shows a signature of magnetic reconnection at 18:40 UT as represented by the anti-sunward reversal of the magnetic field direction and the plasma jet reaching a speed of nearly 1000 km s^{-1}. The detailed structure of the current sheet in this event is presented in Nakamura et al. (2006). We focus on two time intervals with large wave activity in the neighborhood of the magnetic field reversal: 18:38:00–18:40:00 UT (Interval 1) and 18:40:40–18:42:40 UT (Interval 2). The four Cluster spacecraft form a nearly regular tetrahedron with an inter-spacecraft distance of about 200 km, ideal for studying waves at wavelengths down to about 0.1 ion inertial lengths. Interval 1 is characterized by an ion beta of 0.26, a mean flow of 214 km s^{-1} with variation of about 142 km s^{-1}, a mean magnetic field of 20.7 nT with variation of about 4.7 nT, an ion density of about 0.10 cm^{-3}, and an ion temperature of about 33 MK. Interval 2 features an ion beta of 0.40, a mean flow of 740 km s^{-1} with variation of about 216 km s^{-1}, a mean magnetic field of 19.1 nT with variation of about 5.5 nT, an ion density of about 0.08 cm^{-3}, and an ion temperature of about 54 MK. The field reversal measured at about 18:40 UT suggests a thin current sheet with a half-width of about 220 km, the same scale as Cluster's tetrahedral configuration. The inertial lengths are about $d_\mathrm{i} = 2\pi V_\mathrm{A}/\Omega_\mathrm{p} = 3197$ km (where V_A and Ω_p denote the Alfvén speed and the proton gyrofrequency) and $d_\mathrm{e} = 70$ km, and the gyroradii are about $r_\mathrm{p} = 2\pi v_\mathrm{th(p)}/\Omega_\mathrm{p} = 3523$ km (with the proton thermal speed $v_\mathrm{th(p)}$) and $r_\mathrm{e} = 82$ km for protons and electrons, respectively, in the region of intervals 1 and 2.

2.2 Four-dimensional wave spectra

Four-point fluxgate magnetometer data are used to evaluate the energy spectra for the fluctuations in the two intervals directly in the Fourier domain spanning the spacecraft-frame frequencies ω and the three components of the wavevectors $[k_{\perp 1}, k_{\perp 2}, k_\parallel]$ in the mean-field-aligned (MFA) coordinate system, with the basis vectors,

$$[\boldsymbol{e}_{\perp 1}, \boldsymbol{e}_{\perp 2}, \boldsymbol{e}_\parallel] = [(\boldsymbol{e}_B \times \boldsymbol{e}_U) \times \boldsymbol{e}_B, \boldsymbol{e}_B \times \boldsymbol{e}_U, \boldsymbol{e}_B],$$

using the directions of the mean flow $\boldsymbol{e}_U$ and the mean magnetic field $\boldsymbol{e}_B$.

To obtain the spectra, the time series data are transformed into the frequency domain at each spacecraft using the fast Fourier transform, and the set of the frequency spectra is then projected onto the three-dimensional wavevector domain using the wave telescope or minimum variance operator (which is equivalent to the maximum likelihood method assuming a Gaussian likelihood function) (Glassmeier et al., 2001) and the eigenvector analysis of the cross spectral density matrix (Schmidt, 1986; Narita et al., 2011).

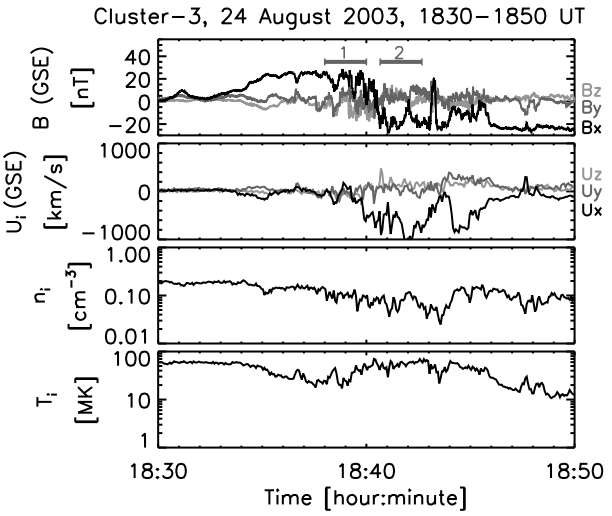

Figure 1. Time series plot of the magnetic field, the ion bulk velocity, the ion number density, and the ion temperature measured by Cluster-3 spacecraft. Data are obtained by fluxgate magnetometers (Balogh et al., 2001) and electrostatic ion analyzers (Rème et al., 2001).

It is worth mentioning that the projection method used here only assumes that the fluctuating field represents a set of plane waves and isotropic noise, and the spectra are determined by minimizing the isotropic noise. Therefore, the spectra are obtained without being biased from Taylor's frozen-in flow hypothesis, specific wave modes, or wavevector anisotropies.

The four-dimensional spectra are displayed for the fluctuations in intervals 1 (Fig. 2) and 2 (Fig. 3) in a six-panel format by averaging over the wavevector components orthogonal to the panel and integrating over the frequencies. We identify the following similarities and differences between the two intervals. The similarities are found in (1) the continuous and smooth distribution of the fluctuation energy, (2) the dominance of the fluctuation energy at the lowest frequencies and the smallest wavenumbers, (3) the overall monotonous decay of the fluctuation energy at increasing frequencies and wavenumbers, (4) wavevector anisotropy with a spectral extension in the perpendicular direction to the mean magnetic field, and (5) the breakdown of axial symmetry in the directions around the mean field. The differences are found in the Interval-2 spectrum in (1) the existence of the spectral extension in the plane spanning the parallel component of the wavevectors and the frequencies (top right panel in Fig. 3) and (2) the moderate offset of the spectral extension from the perpendicular direction in the plane spanning the perpendicular-1 and parallel components of the wavevectors (bottom left panel). The properties of the wavevector spectra

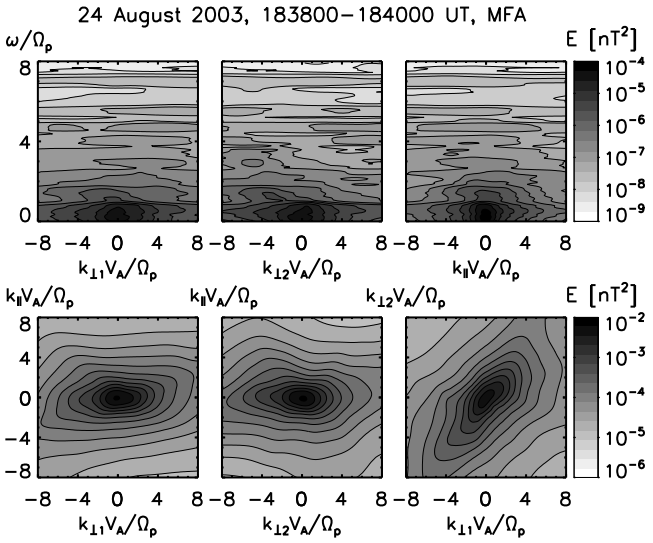

Figure 2. Four-dimensional magnetic energy spectrum on Interval 1 projected (by combining the frequency integration and averaging over the wavevector components) onto three planes spanning the wavevector components and the spacecraft-frame frequencies (top three panels) and three planes spanning the wavevector components. The frequencies and the wavevector components are normalized to the proton gyrofrequency and the proton inertial length, respectively.

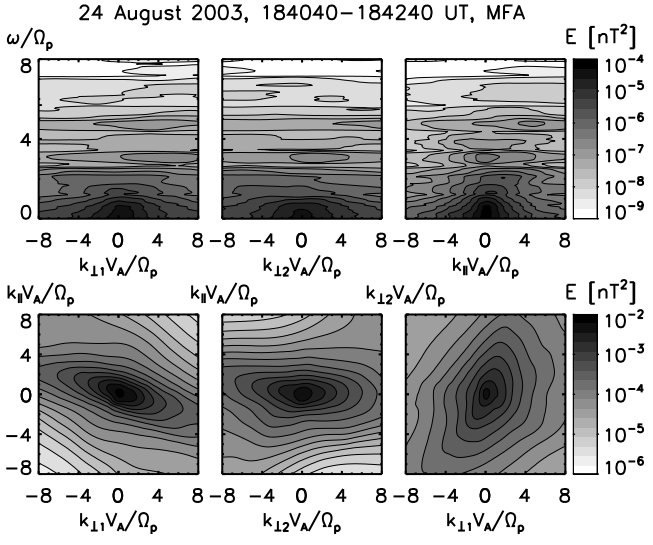

Figure 3. Projection of the energy spectrum on Interval 2 (format of panels the same as in Fig. 2).

are reminiscent of plasma turbulence in that many coexisting waves organize an anisotropic wavevector spectrum and a monotonous spectral decay. The spectral extension in the parallel wavenumber-frequency domain on Interval 2 represents the Doppler shift due to the flow (the flow direction is nearly aligned with the parallel direction).

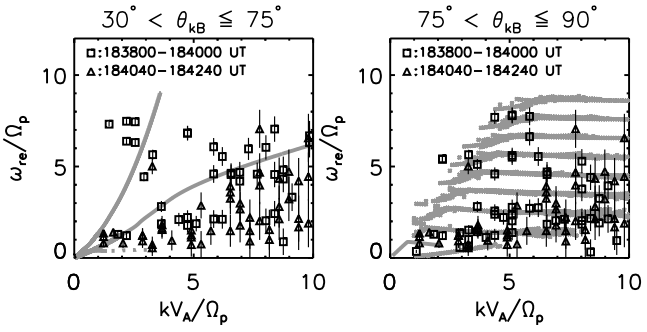

Figure 4. Distribution of the wave frequencies in the plasma rest frame and the wavevector magnitudes for the local peaks of the four-dimensional energy spectra for different groups of wavevector angles from the mean magnetic field. Left panel, top to bottom: dispersion relations from the linear Vlasov theory are shown in gray for the whistler, kinetic slow, and the ion cyclotron modes for ion beta $\beta_i = 0.3$ and the median wavevector angle $\theta_{kB} = 50°$; right panel: the ion Bernstein modes (at harmonics of the ion gyrofrequency) and kinetic Alfvén mode (at the lowest frequencies) at the angle $\theta_{kB} = 85°$.

2.3 Dispersion relation

The wave modes are studied by comparing the diagram of dispersion relation between the measurement and the linear Vlasov theory. The measured dispersion diagrams are obtained by selecting the local peaks in the energy spectra and plotting the frequencies in the rest frame of the plasma (comoving with the bulk flow), ω_{re}, as a function of the wavevector magnitudes. The dispersion diagrams are obtained for two distinct groups of propagation angles: (1) oblique directions from the mean magnetic field $30° < \theta_{kB} \leq 75°$ (left panel in Fig. 4) and (2) quasi-perpendicular directions $75° < \theta_{kB} \leq 90°$ (right panel in Fig. 4). The reason for the classification into the two groups is that in the linear Vlasov theory, the ion Bernstein modes appear as bifurcated branches of the whistler mode at frequencies around the ion gyrofrequency (the fundamental mode) and its harmonics at propagation angles above 75° and the ion cyclotron mode turns into the kinetic Alfvén mode. The theoretical dispersion relations are obtained under the conditions of an ion beta of $\beta_i = 0.3$ (representative of ion beta over the two analyzed intervals), propagation angles of $\theta_{kB} = 50$ and 80° (which are the median of the wave groups 1 and 2, respectively), and a moderately weak damping, $|\gamma/\omega| \leq 0.5$, where γ is the damping rate (strongly damped wave is shown in a dotted curve in the left-hand panel of Fig. 4 for the ion cyclotron mode).

The observationally determined dispersion diagram shows a rather poor agreement with the theoretical modes in the oblique propagation directions (up to 75°) but a good agreement with the ion Bernstein waves (in particular, the second harmonic modes of the proton gyrofrequency) in the quasi-perpendicular direction (above 75°) within the error bars (estimated for the variation in the flow velocities). No

clear agreement is seen with the fundamental mode of the ion Bernstein waves due to strong damping at wavenumbers $kV_A/\Omega_p \geq 2$. Also, only a small portion of the measured waves can be explained by the whistler, the kinetic slow, the ion cyclotron, or the kinetic Alfvén modes. Most of the measured frequencies at high wavenumbers are limited to several proton gyrofrequencies in both wave groups. In the oblique directions, the measured frequencies are too low to explain by the whistler or the kinetic slow mode and too high to explain by the ion cyclotron mode (in addition to the fact that the ion cyclotron mode is strongly damped for $kV_A/\Omega_p \geq 2$).

3 Conclusion and discussion

The measurement of the four-dimensional energy spectra and the dispersion diagram provides new insight into the waves in reconnecting magnetic fields on spatial scales smaller than the ion inertial length. The energy spectra are anisotropic and axially asymmetric in the wavevector domain, showing an extension in the perpendicular direction to the mean magnetic field. The dispersion diagram shows an indication of the ion Bernstein waves though the measured frequencies are somewhat scattered or deviate from the theoretical ones.

In our measurements, the ions can be in resonance with the Bernstein waves at the second harmonic and above because the ratio of the gyroradius to the inertial length is about 0.5. The wave is strongly damped at the fundamental mode, and this fact agrees with the dispersion diagram obtained from the Cluster data. Judging from the existence of an ion burst flow during the analyzed intervals, we conclude that the Bernstein waves likely exist in an ion outflow region.

Ion Bernstein waves may cause a bifurcation of the current sheet in the reconnection outflow region through the Landau–Ginzburg-type transition (Guo and Wang, 2015; Treumann and Baumjohann, 2015) and may contribute to a slow reconnection process through the anomalous resistivity. In the magnetotail plasma, however, electron-scale physics in a thin current sheet leads to a fast reconnection process (Treumann and Baumjohann, 2015). We conclude by noting the importance of waves in studying reconnection, e.g., to see how often the ion Bernstein waves appear in a reconnection region or if the Bernstein waves can coexist with the other modes that likely exist in the reconnection region such as the lower hybrid drift waves (or modified two-stream instability) and the whistler waves. These tasks require spectral analysis at higher frequencies and higher wavenumbers; this will be made possible on scales of electron gyration by the MMS (Magnetospheric Multi-Scale) mission.

Acknowledgements. Y. Narita thanks R. A. Treumann for helpful discussions and suggestions during the preparation of the manuscript. The work by K.-H. Glassmeier is financially supported by the German Bundesministerium für Wirtschaft und Energie and the Deutsches Zentrum für Luft- und Raumfahrt under contract 50 OC 1402. The work by U. Motschmann and H. Comişel is supported by Collaborative Research Center 963, *Astrophysical Flow, Instabilities, and Turbulence*, of the German Science Foundation. The work conducted in Bucharest is supported by the Romanian Ministry for Scientific Research and Innovation, CNCS – UEFISCDI, PN-II-RU-TE-2014-4-2420, *Studiu multi-scala al turbulentei in plasme astrofizice*.

The topical editor, E. Roussos, thanks one anonymous referee for help in evaluating this paper.

References

Balogh, A., Carr, C. M., Acuña, M. H., Dunlop, M. W., Beek, T. J., Brown, P., Fornacon, K.-H., Georgescu, E., Glassmeier, K.-H., Harris, J., Musmann, G., Oddy, T., and Schwingenschuh, K.: The Cluster Magnetic Field Investigation: overview of in-flight performance and initial results, Ann. Geophys., 19, 1207–1217, doi:10.5194/angeo-19-1207-2001, 2001.

Eastwood, J. P., Phan, T. D., Bale, S. D., and Tjulin, A.: Observations of turbulence generated by magnetic reconnection, Phys. Rev. Lett., 102, 035001, doi:10.1103/PhysRevLett.102.035001, 2009.

Escoubet, C. P., Fehringer, M., and Goldstein, M.: *Introduction*, The Cluster mission, Ann. Geophys., 19, 1197–1200, doi:10.5194/angeo-19-1197-2001, 2001.

Fujimoto, K. and Sydora, R. D.: Whistler waves associated with magnetic reconnection, Geophys. Res. Lett, 35, L19112, doi:10.1029/2008GL035201, 2008.

Glassmeier, K.-H., Motschmann, U., Dunlop, M., Balogh, A., Acuña, M. H., Carr, C., Musmann, G., Fornaçon, K.-H., Schweda, K., Vogt, J., Georgescu, E., and Buchert, S.: Cluster as a wave telescope –first results from the fluxgate magnetometer, Ann. Geophys., 19, 1439–1447, doi:10.5194/angeo-19-1439-2001, 2001.

Guo, Z. and Wang, X.: Onset of fast magnetic reconnection via subcritical bifurcation, Front. Phys., 3, 18, doi:10.3389/fphy.2015.00018, 2015.

Nakamura, R., Baumjohann, W., Asano, Y., Runov, A., Balogh, A., Owen, C. J., Fazakerley, A. N., Fujimoto, M., Klecker, B., and Rème, H.: Dynamics of thin current sheets associated with magnetotail reconnection, J. Geophys. Res., 111, A11206, doi:10.1029/2006JA011706, 2006.

Narita, Y., Glassmeier, K.-H., and Motschmann, U.: High-resolution wave number spectrum using multi-point measurements in space – the Multi-point Signal Resonator (MSR) technique, Ann. Geophys., 29, 351–360, doi:10.5194/angeo-29-351-2011, 2011.

Norgren, C., Vaivads, A., Khotyaintsev, Y. V., and Andrè, M.: Lower hybrid drift waves: space observations, Phys. Rev. Lett., 109, 055001, doi:10.1103/PhysRevLett.109.055001, 2012.

Rème, H., Aoustin, C., Bosqued, J. M., Dandouras, I., Lavraud, B., Sauvaud, J. A., Barthe, A., Bouyssou, J., Camus, Th., Coeur-Joly, O., Cros, A., Cuvilo, J., Ducay, F., Garbarowitz, Y., Medale, J.

L., Penou, E., Perrier, H., Romefort, D., Rouzaud, J., Vallat, C., Alcaydé, D., Jacquey, C., Mazelle, C., d'Uston, C., Möbius, E., Kistler, L. M., Crocker, K., Granoff, M., Mouikis, C., Popecki, M., Vosbury, M., Klecker, B., Hovestadt, D., Kucharek, H., Kuenneth, E., Paschmann, G., Scholer, M., Sckopke, N., Seidenschwang, E., Carlson, C. W., Curtis, D. W., Ingraham, C., Lin, R. P., McFadden, J. P., Parks, G. K., Phan, T., Formisano, V., Amata, E., Bavassano-Cattaneo, M. B., Baldetti, P., Bruno, R., Chionchio, G., Di Lellis, A., Marcucci, M. F., Pallocchia, G., Korth, A., Daly, P. W., Graeve, B., Rosenbauer, H., Vasyliunas, V., McCarthy, M., Wilber, M., Eliasson, L., Lundin, R., Olsen, S., Shelley, E. G., Fuselier, S., Ghielmetti, A. G., Lennartsson, W., Escoubet, C. P., Balsiger, H., Friedel, R., Cao, J.-B., Kovrazhkin, R. A., Papamastorakis, I., Pellat, R., Scudder, J., and Sonnerup, B.: First multispacecraft ion measurements in and near the Earth's magnetosphere with the identical Cluster ion spectrometry (CIS) experiment, Ann. Geophys., 19, 1303–1354, doi:10.5194/angeo-19-1303-2001, 2001.

Schmidt, R. O.: Multiple emitter location and signal parameter estimation, IEEE Trans. Ant., Prop., AP-34, 276–280, doi:10.1109/TAP.1986.1143830, 1986.

Treumann, R. A.: Origin of resistivity in reconnection, Earth Planet Space, 53, 453–462, doi:10.1186/BF03353256, 2001.

Treumann, R. A. and Baumjohann, W.: Broad current sheets, current bifurcation, and collisionless reconnection – An Opinion on "Onset of fast magnetic reconnection via subcritical bifurcation" by Guo, Z. and Wang, X., Front. Phys., 3, 40, doi:10.3389/fphy.2015.00040, 2015.